Distinctive tasks of different cyanobacteria and associated bacteria in carbon as well as nitrogen fixation and cycling in a late stage Baltic Sea bloom

Falk Eigemann[1*], Angela Vogts[1], Maren Voss[1], Luca Zoccarato[2], Heide Schulz-Vogt[1]

1 Leibniz Institute for Baltic Sea Research Warnemünde, Department of Biological Oceanography, 18119 Rostock, Germany

[2] Leibniz-Institute for Freshwater Ecology and Inland Fisheries, Department of Stratified Lakes, Alte Fischerhütte 2, OT Neuglobsow, 16775 Stechlin, Germany

*falkeigemann@gmail.com, phone: 0049-381-51973462, fax: 0049-381-5197-211

Short title: Distinctive tasks in cyanobacterial blooms

Abstract

Cyanobacteria and associated heterotrophic bacteria hold key roles in carbon as well as nitrogen fixation and cycling in the Baltic Sea due to massive cyanobacterial blooms each summer. The species specific activities of different cyanobacterial species as well as the N- and C-exchange of associated heterotrophic bacteria in these processes, however, are widely unknown. Within one time series experiment we tested the cycling in a natural, late stage cyanobacterial bloom by adding ^{13}C bi-carbonate and $^{15}N_2$, and performed sampling after 10 min, 30 min, 1 h, 6 h and 24 h in order to determine the fixing species as well as the fate of the fixed carbon and nitrogen in the associations. Uptake of ^{15}N and ^{13}C isotopes by the most abundant cyanobacterial species as well as the most abundant associated heterotrophic bacterial groups was then analysed with a NanoSIMS. Overall, the filamentous, heterocystous species *Dolichospermum* sp., *Nodularia* sp., and *Aphanizomenon* sp. revealed no or erratic uptake of carbon and nitrogen, indicating mostly inactive cells. In contrary, non-heterocystous *Pseudanabaena* sp. dominated the nitrogen and carbon fixation, with uptake rates up to 1.49 ± 0.47 nmol N h^{-1} l^{-1} and 2.55 ± 0.91 nmol C h^{-1} l^{-1}. Associated heterotrophic bacteria dominated the subsequent nitrogen cycling with uptake rates up to 1.2 ± 1.93 fmol N h^{-1} cell $^{-1}$, but were also indicative for fixation of di-nitrogen.

1. Introduction

Cyanobacterial mass occurrences are a worldwide phenomenon in limnic, brackish and marine systems. In the Baltic Sea, such blooms occur regularly during summer [1], and due to their high biomasses they significantly add to eutrophication [2,3]. The onset of blooms is promoted by rising water temperatures and low N:P ratios after N-depletion due to the capability of atmospheric nitrogen fixation by several cyanobacterial species [1,3,4]. Total cyanobacterial nitrogen fixation in the Baltic Sea was estimated with 370 kt yr^{-1} [2], and may

47 contribute up to 55% of total nitrogen input [5,6]. Furthermore, filamentous cyanobacteria
48 may contribute for 44% of the community primary production [7]. The major part of nitrogen
49 and carbon fixation is performed in the early summer, followed by a peak in biomass, and
50 ultimately the decay of the bloom in which predominantly recycling processes occur [6,8].
51 Cyanobacteria as well as eukaryotic phytoplankton live in close associations with
52 heterotrophic bacteria, and interactions between them may range from symbiosis to
53 competition [9,10]. These interactions strongly influence carbon and nutrient cycling and
54 therewith the stability of aquatic food webs [11, 12]. In phytoplankton blooms, heterotrophic
55 bacteria may provide macronutrients via recycling (or fixation) but may be also competitors
56 for inorganic nutrients [11]. Especially at the late stages of cyanobacterial blooms, the
57 associated heterotrophic bacteria may be responsible for a significant share of elemental
58 cycling and fluxes, i.e. for the input of nutrients and organic matter in the ecosystem due to
59 remineralization. Studies on the role of associated bacteria at these late cyanobacterial bloom
60 stages, however, are lacking.
61 The predominant cyanobacterial genera in Baltic Sea blooms are *Aphanizomenon*, *Nodularia*,
62 *Dolichospermum*, *Pseudanabaena* and *Synechococcus*, whereby the dominant groups and
63 species may differ between years and stage of the bloom [12]. The first three mentioned
64 genera are filamentous and heterocystous, and may form dense surface scums [1]. Baltic Sea
65 *Synechococcus* sp. and *Pseudanabaena* sp. are supposed to be not capable of nitrogen fixation
66 and hence depend on dissolved nitrogen sources [13,14], even though nitrogenase genes occur
67 in *Pseudanabaena* [14,15]. Thus, *Aphanizomenon*, *Nodularia*, and *Dolichospermum* are
68 thought to dominate the biological nitrogen input into the Baltic Sea [14]. Recently, however,
69 heterotrophic bacteria were shown to be capable of nitrogen fixation at depth in the central
70 Baltic Sea [16] and may even be the principle N_2 fixing organism in a Baltic Sea estuarine
71 [17]. However, studies that examined carbon and nitrogen fixation in cyanobacterial blooms
72 and associated heterotrophic bacteria mostly focussed on single cyanobacterial species [7,18],

or neglected associated bacteria as well as the fate of the fixed carbon and nitrogen in the associations [14]. In the present study, we incubated a natural late stage Baltic Sea cyanobacterial bloom with ^{13}C bi-carbonate and $^{15}N_2$, and followed the uptake over time by means of NanoSIMS technique. Therewith, we aimed at unravel the specific contribution of different cyanobacterial species and associated heterotrophic bacteria in carbon and nitrogen fixation as well as the fate of the fixed carbon and nitrogen in the associations.

2. Material and Methods

2.1. Incubation experiments:

A natural cyanobacterial bloom was sampled at station TransA (58°43.8`N, 18°01.9`E, Fig. 1) on 13.08.2015. Bloom samples were further concentrated by means of a light trap to remove positive phototactic zooplankton until a cyanobacterial chl. a concentration of 9 µg l^{-1} was reached (measured with a PHYTO-PAM, Heinz Walz GmbH). At Askö laboratory (ca. 1 h transfer), five 176 mL opaque Nalgene bottles were filled with the concentrated bloom till overflowing and sealed with septum caps enabling addition and retrieval of liquids with syringes.

Figure 1: True color satellite image of a cyanobacterial bloom in the Baltic Sea on August 13, 2015 derived from MODIS/Terra (NASA/GSFC, Rapid Response). The arrow in the zoom image on the right side points towards the sampling station TransA.

For ^{15}N addition, 1 mL of the sample was removed and subsequently 1 mL 99% pure $^{15}N_2$ gas injected with a syringe, resulting in 31.68 atom % ^{15}N. For amending ^{13}C, 5 ml sample were removed with a syringe and subsequently 5 ml F/2 medium [52] without nitrogen source, adjusted to 8 PSU and spiked with 0.4 g $NaH^{13}CO_3$ added (final concentration 108.36 atom % ^{13}C). Incubation times were 10 min, 30 min, 1 h, 6 h and 24 h. Bottles were incubated in an

97 incubation chamber at 16.5 ± 0.5 °C at approximately 60 µmol photons s^{-1} m^{-2} (delivered from
98 ROHS 36W 840 light bulbs), resembling the natural conditions of sampling under constant
99 light (Supplemental 1).
100

101 ## 2.2. Sampling

102 Each sample was fixed with formaldehyde (2% final concentration) for 3 h in the dark at
103 room temperature, and filtered gently onto 3 µm pore width polycarbonate filters for later
104 inspection with CARD-FISH and NanoSIMS. Before start of the incubation, 80 mL of the
105 stock sample were filtered onto 3 µm pore width polycarbonate filter for DNA extraction of
106 the associated bacterial fraction. For phytoplankton counting, a 100 mL subsample was fixed
107 with an acidic Lugol solution [19] and counted according to the Utermöhl technique. To
108 determine biomass percentages, the carbon content (µg l^{-1}) of each species was calculated
109 using the official PEG Biovolume Report 2016 (International Council for the Exploration of
110 the Sea) for phytoplankton species and the carbon content per counting unit for the respective
111 size class.
112

113 ## 2.3. DNA extraction

114 DNA was extracted as described in [20] with modifications. Briefly, the filters were cut into
115 pieces and mixed with sterilized zirconium beads, 500 µl of phenol/chloroform mix, and 500
116 µl of SLS extraction buffer. After centrifugation of the mixture, the supernatant was
117 transferred to another tube and the process was repeated. DNA was precipitated overnight at
118 −20°C. The pellet was washed with ethanol, dried, and resolved in autoclaved DEPC-treated
119 water.
120

121 2.4. PCR and sequencing

122 For PCRs, 10 ng of DNA was added to autoclaved DEPC-treated water, 10× PCR buffer,
123 BSA, $MgCl_2$, dNTPs, forward and reverse primers, and native Taq polymerase. Bacterial
124 DNA was amplified using the primers 341f and 805r [21], under the following conditions: 30
125 cycles of denaturation for 40 s at 95°C, 40 s of annealing at 53°C, and 1 min of elongation at
126 72°C. PCR products were cleaned with the Nucleospin kit following the manufacturer's
127 instructions and shipped to LGC Genomics GmbH (Berlin). Illumina MiSeq V3 sequencing
128 with 300 bp paired-end reads was performed using the 16S primers 341F and 785R. The
129 forward and reverse reads were deposited at the European Nucleotide Archive under the
130 accession number PRJEB23316 (sample B15_3). Taxonomic identification of the associated
131 bacterial community, was performed as described in [22] with the NGS analysis pipeline of
132 the SILVA rRNA gene database project (SILVAngs 1.3).

133

134 2.5. CARD-FISH analyses

135 The Illumina runs mostly yielded Alphaproteobacteria and Cytophaga/Bacteroidetes (Fig. 3),
136 and probes Alf968 [23] and CF968 [24] were chosen for analyses of associated heterotrophic
137 bacteria. CARD FISH analyses were computed as described in [25] with modifications: Filter
138 pieces were doused in 0.2 % fluid agarose, dried, and subsequently incubated for 60 min at 37
139 °C in 10 mg ml^{-1} lysozym solution and thereafter for 15 min at 37 °C with achromopeptidase
140 (180 U ml^{-1}). For inactivation, filter pieces were doused subsequently to 1x PBS, autoclaved
141 MilliQ and 99% ethanol and following placed for 10 min in 0.01 M HCl at room temperature.
142 Hybridization with horseradish peroxidase labeled 16S rRNA probes Alf968 and CF968 were
143 carried out at 35 °C with 55% formamide for 3.5 and 4 h, respectively. Signal amplification
144 was achieved with Oregon green 488-X bound to tyramide as described in [26]. After

145 hybridization, filter pieces were stained with 4,6-diamidin-2-phenylindol (DAPI) solution for
146 unspecific counter-staining of all cells.

147

148 2.6. Laser-Scanning Microscope, Scanning electron microscope and sputtering

149 Spots of interest were determined by fluorescence microscopy and subsequently laser marked
150 with a laser microdissectional microscope. For confirmation of associated bacteria and
151 cyanobacterial species, SEM analyses were performed. Therefore, filter pieces were covered
152 with approximately 8 nm gold in a sputter coater (Cressington108 auto-sputter coater).
153 Samples were analyzed with a Scanning electron microscope (Zeiss Merlin VP compact) with
154 the Zeiss Smart SEM Software. Before NanoSIMS analyses, filter pieces were covered with
155 ca. 30 nm additional gold with a sputter coater (see above).

156

157 2.7. NanoSIMS measurements

158 SIMS imaging was performed using a NanoSIMS 50L instrument (Cameca, France). A $^{133}Cs^{+}$
159 primary ion beam was used to erode and ionize atoms of the sample. Among the received
160 secondary ions, images of $^{12}C^{-}$, $^{13}C^{-}$, $^{12}C^{14}N^{-}$ and $^{12}C^{15}N^{-}$ were recorded simultaneously for
161 cells at the laser microdissectional (LMD)-marked spots using electron multipliers as
162 detectors. The mass resolving power was adjusted to suppress interferences at all masses
163 allowing, e.g. the separation of $^{12}C^{15}N^{-}$ from interfering ions such as $^{13}C^{14}N^{-}$. Prior to the
164 analysis, sample areas of 30×30 µm were sputtered for 2 min with 600 pA to erode the gold
165 and reach the steady state of secondary ion formation. The primary ion beam current during
166 the analysis was 1 pA; the scanning parameters were 512×512 px for areas of 20–30 µm, with
167 a dwell time of 250 µs per pixel.

168

2.8. Analyses of NanoSIMS measurements

All NanoSIMS measurements were analysed with the Matlab based program look@nanosims [27]. Briefly, the 60 measured planes were checked for inconsistencies and all usable planes accumulated, regions of interest (i.e. cells of cyanobacterial filaments, associated bacterial cells and filter regions without organic material for background measurements) defined based on $^{12}C^{14}N$ mass pictures, and $^{13}C/^{12}C$ as well as $^{15}N/^{14}N$ ratios calculated from the ion signals for each region of interest. Measurements of heterocysts in *Aphanizomenon* sp., *Dolichospermum* sp., and *Nodularia* sp. were avoided due their specific cell metabolism. For analyses of each measurement, first the means of background measurements were determined, and this mean factorized for theoretical background values (0.11 for $^{13}C/^{12}C$ and 0.00367 for $^{15}N/^{14}N$). These factors were applied to all non-background regions of interest in the same measurement. For each time-point, values for each species (or bacterial group for the associated bacteria) were pooled (i.e. different cells in one measurement as well as different measurements) and means for each species (or bacterial group for the associated bacteria) for each time-point calculated. Work flow for an example spot from Card-FISH to NanoSIMS analyses is illustrated in Fig. 2. The numbers of measured cells per species/group and time point, as well as overall measured areas per time point are given in Supplemental 2.

Figure 2: Work flow for analyses of cyanobacteria and their associated heterotrophic bacteria. A: Card-FISH image of a *Nodularia* sp. filament with two associated Alphaproteobacteria taken with a laser microdissectional microscope. The marking arrow can be seen at the right side. B: Scanning electron microscope image of the same spot for confirmation of associated bacteria (middle-right side of the filament) and identification of *Nodularia* sp. The tip of the marking arrow can be seen at the right side of the image. C: accumulated NanoSIMS images of the same spot with blue (low) to red (high) ^{15}N signal (as example). The circled areas

194 display the regions of interest, whereof $^{13}C/^{12}C$ and $^{15}N/^{14}N$ ratios were calculated. Control
195 (filter without cyanobacteria or heterotrophic bacteria) regions can be seen at the top-right and
196 down-left, *Nodularia* sp. regions are displayed in the bluish part, and the associated
197 Alphaproteobacteria by the smaller regions in the reddish part of the image.

198

199 2.9. Uptake rates of ^{13}C and ^{15}N

200 Uptake rates for nitrogen and carbon were calculated as described in [28] according to the
201 equation:

202 $$V(T^{-1}) = (1/\Delta_t)\ ((A_{PNf} - A_{PN0})/(A_{N2} - A_{PN0})),$$

203 where A_{N2} is the ^{15}N or ^{13}C enrichment of the N or C available for fixation; A_{PN0} the ^{15}N or
204 ^{13}C enrichment of particulate N or C at the start of the experiment; A_{PNf}, the ^{15}N or ^{13}C
205 enrichment of particulate N or C at the end of the experiment; and

206 $$p(M\ L^{-3}\ T^{-1}) = V/2 * PX,$$

207 where PX is the concentration of N or C for the respective cyanobacterial species in the
208 incubation bottles, or the cellular N or C content for the associated bacteria. The solubility of
209 N and C was calculated using the Excel Sheet provided by Joe Montoya, based on [29] for
210 CO_2 and [30] for N_2. For cyanobacteria gross uptake rates were calculated per volume and
211 time, and for the associated bacteria per cell and time, because no absolute numbers of
212 associated bacteria were existent. The C:N ratios in the cyanobacteria were assumed with 6.3
213 [14,31]. The size of the associated bacteria was assumed with 2x1 µm (SEM analyses), the
214 carbon content with 0.35 pg C μm^{-3} [32], and the C:N ratio with 5:1 [33]. We are aware that
215 the used "bubble-method" for injection of N_2 gas assumes an instantaneous equilibrium
216 between the $^{15}N_2$ gas bubble and the N_2 dissolved in water, which in fact may be time-delayed
217 [34], and ultimately leads to an underestimation of fixation rates. Thus, especially at the early

218 measuring points (10 and 30 min), the calculated rates should be considered as proxy values
219 with percentage errors up to 70% [35].

220

221 2.10. Data analyses

222 All data were analysed with R studio [36]. To test for differences in stable isotope ratios
223 between species/groups or between different time-points in the same group/species,
224 ANOVAS (analyses of variance) with subsequent Tukey HSD posthoc tests with the package
225 agricolae were performed. Likewise, the impact of the host species on the stable isotope
226 uptake of the associated bacteria was tested with ANOVAs, by comparing associated bacterial
227 cells from different hosts. Possible cell-to-cell transfer of ^{13}C and ^{15}N between host and
228 associated bacteria were tested by calculating linear models of $^{13}C/^{12}C$ and $^{15}N/^{14}N$ ratios
229 between the host cells and the associated bacterial cells for each incubation period. To test for
230 correlations between ^{13}C and ^{15}N uptake, linear models were calculated with the lm function.
231 To test for differences in relations of ^{13}C to ^{15}N uptake between species/groups, dissimilarity
232 matrices (horn distances) were calculated with a xy ($x = ^{13}C/^{12}C$, $y = ^{15}N/^{14}N$) system, and
233 subsequently ANOSIM analyses performed with the vegan package. To test for differences in
234 $^{13}C/^{15}N$ uptake relations between functional groups, ANCOVAs with and without interactions
235 between the factor and the co-variable were calculated with linear models. Here, ^{13}C uptake
236 was set as dependent variable, ^{15}N uptake as co-variable, and the functional group as factor.
237 Next, ANOVAs were calculated for both ANCOVAs to test for differences in the slopes of
238 the linear models.

239

240 3. Results

241 3.1. Community composition of the phytoplankton and associated bacteria

The phytoplankton community was dominated by the cyanobacteria *Aphanizomenon* sp. (33% biomass), *Nodularia* sp. (30% biomass), *Pseudanabaena* sp. (9% biomass) and *Dolichospermum* sp. (8% biomass), which together accounted for 80% of the total biomass (Figure 3a). The most abundant associated bacteria belonged to Alphaproteobacteria (39%), Cytophaga/Bacteroidetes (20%), Gammaproteobacteria (18%), Verrucomicrobia (6%), Planctomycetes (5%), Betaproteobacteria (4%) and Actinobacteria (1%, Fig. 3b).

Figure 3. A: Pie chart for the most abundant phytoplankton groups (left side, in % biomass). B: Pie chart for the most abundant bacterial groups (right side, in % of sequencing reads).

The general appearance of the bloom (Fig. 4a), and microscopy of cyanobacteria (Fig. 4b-e) both indicated a late stage of the bloom (especially the "curly" appearance of *Nodularia* sp.), with many associated bacteria to the heterocystous species (Fig. 4f).

Figure 4. Appearance of the bloom at the day of sampling (a), and microscopic images of *Pseudanabaena* sp. (b), *Aphanizomenon* sp. (c), *Nodularia* sp. (d), *Dolichospermum* sp. (e), and a DAPI stained sample with *Nodularia* sp. and associated bacteria.

3.2. Bi-carbonate uptake of cyanobacteria and associated heterotrophic bacteria

Significant differences in the ^{13}C incorporation between the bacterial groups were observed at all sampling points (Fig. 5). *Pseudanabaena* sp. showed the highest $^{13}C/^{12}C$ ratios at all sampling points with continuously increasing incorporation of ^{13}C over time. At the early time points (10, 30 and 60 min), all other species/groups displayed a $^{13}C/^{12}C$ ratio close to the natural occurring value of 0.011 (Fig. 5). After 6 and 24 h of incubation, however, Cytophaga/Bacteroidetes revealed the second highest $^{13}C/^{12}C$ ratios, corresponding to significant ^{13}C enhancements with a more than two- and ten-fold increase of the natural occurring ratio after 6 and 24 h, respectively (Fig. 5). Mentionable, the filamentous

Species/incubation time	**10 min**	**30 min**	**60 min**	**6 h**	**24 h**
			^{13}C uptake nmol C h^{-1} l^{-1} (fmol C h^{-1} cell $^{-1}$ for associated bacteria)		
Aphanizomenon sp.	0.3 ± 3.52	0.00 ± 0.57	1.06 ± 2.69	0.41 ± 1.35	0.00 ± 0.02
Dolichospermum sp.	0.06 ± 0.76	0.25 ± 0.71	0.05 ± 0.2	0.07 ± 0.13	0.27 ± 0.18
Nodularia sp.	5.88 ± 20.28	0.00 ± 0.95	0.4 ± 1.5	0.19 ± 0.4	0.00 ± 0.03

cyanobacteria *Aphanizomenon* sp., *Dolichospermum* sp. and *Nodularia* sp. did not display elevated $^{13}C/^{12}C$ ratios over the whole 24 h incubation period with two exceptions: *Aphanizomenon* sp. revealed enhanced ratios after 6 h and *Dolichospermum* sp. after 24 h of incubation (data not shown, Fig. 5). To test for a possible impact of the host-species on ^{13}C uptake of the associated bacteria, we compared the $^{13}C/^{12}C$ ratios obtained from Alphaproteo- and Cytophaga/Bacteroidetes bacteria from different host species. In most cases, however, no significant differences occurred between the hosts (ANOVAs, data not shown). Especially in the 6 and 24 h exposures, where increased $^{13}C/^{12}C$ ratios were obtained for both of the associated bacterial groups (Fig. 5), no impact of the host species could be seen (data not shown). Linear models on ^{13}C uptake between the host cells and the associated bacterial cells did not suggest cell-cell transfer of ^{13}C except for the 60 min incubation (R^2 = -0.05, 0.12, 0.24, -0.03, -0.05; p = 0.84, 0.24, 0.01, 0.48, 0.75, for 10 min, 30 min, 60 min, 6 h and 24 h incubation, respectively). The calculated uptake rates of the cyanobacteria were highest for *Pseudanabaena* sp. after 60 min with 2.55 ± 0.91 nmol C h^{-1} l^{-1}, and from the associated bacteria for Cytophaga/Bacteroidetes bacteria with 0.31 ± 0.34 fmol C h^{-1} cell^{-1} after 24 h of incubation (Table 1).

Table 1: Carbon and nitrogen uptake rates ± standard deviation given in nmol C or N h^{-1} l^{-1} for cyanobacteria, and fmol C or N h^{-1} cell^{-1} for associated bacteria.

Pseudanabaena sp.	2.48 ± 1.5	1.98 ± 0.89	2.55 ± 0.91	1.13 ± 0.72	1.87 ± 1.08
Alphaproteo	0.59 ± 0.9	0.00 ± 0.04	0.00 ± 0.07	0.13 ± 0.23	0.2 ± 0.32
Cytophaga/Bacteroidetes	0.12 ± 0.09	0.24 ± 0.45	0.03 ± 0.06	0.19 ± 0.27	0.31 ± 0.34
	^{15}N uptake nmol N h^{-1} l^{-1} (fmol N h^{-1} cell $^{-1}$ for associated bacteria)				
Aphanizomenon sp.	1.03 ± 1.6	0.00 ± 1.27	0.28 ± 0.42	0.17 ± 0.4	0.00 ± 0.02
Dolichospermum sp.	0.73 ± 0.45	0.17 ± 0.3	0.05 ± 0.08	0.09 ± 0.17	0.04 ± 0.03
Nodularia sp.	8.07 ± 18.4	0.03 ± 0.87	0.18 ± 0.53	0.19 ± 0.23	0.00 ± 0.02
Pseudanabaena sp.	1.49 ± 0,47	0.8 ± 0.56	0.84 ± 0.17	0.48 ± 0.31	0.17 ± 0.05
Alphaproteo	0.00 ± 0.08	0.2 ± 0.73	0.31 ± 0.76	1.15 ± 1.29	0.34 ± 0.2
Cytophaga/Bacteroidetes	0.95 ± 1.01	0.36 ± 0.53	1.2 ± 1.93	0.67 ± 0.92	0.25 ± 0.17

Figure 5: Boxplots of $^{13}C/^{12}C$ ratios for *Aphanizomenon* sp., *Dolichospermum* sp., *Nodularia* sp., *Pseudanabaena* sp., Alphaproteobacteria and Cytophaga/Bacteroidetes bacteria over time, with square root transformed y axis. Values originate from pooled data for the respective species from different measurements and cells (Supplemental 2). Lower case letters above the boxplots refer to different groups of Tukey HSD Post-Hoc tests. Heterocystous cyanobacteria are displayed in green, non-heterocystous cyanobacteria in blue, and associated heterotrophic bacteria in red.

3.3. $^{15}N_2$ uptake of cyanobacteria and associated heterotrophic bacteria

For all time points, significant differences of ^{15}N incorporation between the species/groups occurred (Fig. 6). After 10 min of incubation, however, all species still showed values around the natural $^{15}N/^{14}N$ ratio of 0.00367 (Fig. 6), whereas after 30 min *Pseudanabaena* sp. (which reveals the highest ^{15}N incorporation), and the associated heterotrophic bacteria showed

299 enhanced $^{15}N/^{14}N$ ratios (Fig. 6). Between 1 and 6 h of incubation especially the
300 Alphaproteobacteria increased their $^{15}N/^{14}N$ ratios, and after 24 h of incubation pronounced
301 differences between the species occured, with associated Alphaproteobacteria showing the
302 highest ^{15}N incorporation (mean = 0.0143 ± 0.0059, almost 4-times increased $^{15}N/^{14}N$ ratios
303 compared to the natural ratio). In general, after 24 h of incubation the associated bacteria
304 revealed the highest ratios, followed by *Pseudanabaena* sp., whereas the heterocystous
305 cyanobacteria displayed even after 24 h of incubation $^{15}N/^{14}N$ ratios close to the natural value
306 (Fig. 6).

307 Figure 6: Boxplots of $^{15}N/^{14}N$ ratios for *Aphanizomenon* sp., *Dolichospermum* sp., *Nodularia*
308 sp., *Pseudanabaena* sp., Alphaproteobacteria and Cytophaga/Bacteroidetes bacteria over time
309 with square root transformed y-axis. Values originate from pooled data for the respective
310 species from different spots and cells (Supplemental 2). Lower case letters above the boxplots
311 refer to different groups of Tukey HSD Post-Hoc tests. Heterocystous cyanobacteria are
312 displayed in green, non-heterocystous cyanobacteria in blue, and associated heterotrophic
313 bacteria in red.

314

315 Comparisons of the $^{15}N/^{14}N$ ratios in each species/group between different incubation times
316 revealed significant ^{15}N incorporation in most species/groups, but inconsistent ^{15}N uptake in
317 the heterocystous species (Fig. 6). In general, the heterocystous cyanobacteria do not display
318 pronounced $^{15}N_2$ uptake over time. In contrast, *Pseudanabaena* sp. displays significantly
319 enhanced $^{15}N/^{14}N$ ratios from 6 h of incubation onwards (Anova, $F = 65.43$, $p < 0.0001$), with
320 steadily increasing values over time and significant differences also between 6 and 24 h of
321 incubation (Fig. 6, Post-Hoc data not shown). Also Alphaproteobacteria and
322 Cytophaga/Bacteroidetes reveal steadily increasing $^{15}N/^{14}N$ ratios over the 24 h incubation
323 period (Anova, $F = 4.87$, $p = 0.003$, and $F = 9.811$, $p < 0.0001$, respectively), with significant

differences between almost all incubation times (Fig. 6, Post-Hoc data not shown). The separation of the obtained $^{15}N/^{14}N$ values of associated Alphaproteo- and Cytophaga/Bacteroidetes bacteria by the host species did not reveal differences between the host species (data not shown). Linear models between the $^{15}N/^{14}N$ ratios of heterocystous cyanobacterial cells that carry associated bacteria and the associated bacteria did not suggest dependencies of ^{15}N uptake between the host and the associated bacterium, with the exception of 30 min incubation (R^2 = -0.02, 0.64, 0.08, -0.03, 0.1; p = 0.48, 0.02, 0.1, 0.39, 0.1 for 10 min, 30 min, 1h, 6 h, and 24 h incubation, respectively). The uptake rates were highest for *Nodularia* sp. with 8.07 ± 18.4 nmol N h^{-1} l^{-1} after 10 min of incubation. However, if excluding the 10 min incubation due to experimental uncertainties, *Pseudanabaena* sp. revealed the highest incorporation rates with 0.84 ± 0.17 nmol N h^{-1} l^{-1} after 1 h of incubation. For the associated bacteria Cytophaga/Bacteroidetes displayed the highest incorporation of ^{15}N with 1.2 ± 1.93 fmol N h^{-1} $cell^{-1}$ after 1 h incubation (Table 1).

3.4. Species- and group specific relations of ^{13}C to ^{15}N uptake

Significant differences between the species/bacterial groups occurred for all time points for relations of ^{13}C against ^{15}N uptake (ANOSIM, each p = 0.001), although different R values were obtained for different exposure times (R = 0.2387, 0.4203, 0.3098, 0.215, 0.585, for 10, 30, 60 min, 6 and 24 h exposure, respectively), indicating most pronounced differences in the relation of ^{13}C to ^{15}N uptake between the species/groups after 24 h of incubation. In general, *Pseudanabaena* sp. was the most noticeable species in the ^{13}C uptake (starting with the 30 min exposure), and the associated Alphaproteo and Cytophaga/Bacteroidetes bacteria in the ^{15}N uptake (starting after 60 min of exposure, Fig. 7). The heterocystous cyanobacteria revealed a high patchiness with few cells displaying prominent ^{13}C uptake (Fig. 5), but mostly did not show obvious uptake of either ^{13}C or ^{15}N (Fig. 7, Table 1). Pooling the different

349 species (for bacteria groups) into the functional groups heterocystous cyanobacteria
350 (*Aphanizomenon* sp., *Dolichospermum* sp., and *Nodularia* sp.), non-heterocystous
351 cyanobacteria (*Pseudanabaena* sp.), and associated bacteria (Alphaproteo- and
352 Cytophaga/Bacteroidetes bacteria), and plotting of the $^{13}C/^{12}C$ and $^{15}N/^{14}N$ ratios against the
353 time, revealed specific tasks of the functional groups (Fig. 7, Table 2). The associated bacteria
354 predominantly display enhanced $^{15}N/^{14}N$ ratios, with the highest ratios after 6 h incubation,
355 whereas non-heterocystous cyanobacteria reveal the highest $^{13}C/^{12}C$ ratios with a time
356 dependent increase. Controversially, only few heterocystous cyanobacteria show increased
357 $^{13}C/^{12}C$ and/or $^{15}N/^{14}N$ ratios (Fig. 7).

358 Figure 7: $^{13}C/^{12}C$ (z axis) and $^{15}N/^{14}N$ (y axis) ratios plotted against the exposure time (log
359 transformed x axis) for the different functional groups (heterocystous cyanobacteria, non-
360 heterocystous cyanobacteria, associated bacteria). The color and symbol legend is given
361 directly in the figure.

362

363 Group specific behavior was corroborated by significantly different slopes between the
364 functional groups in regression analyses of the ^{13}C over ^{15}N uptake for the different exposure
365 times, despite the fact that significant correlations between ^{13}C and ^{15}N uptake occurred for all
366 groups (Table 2). From 60 min of exposure onwards, the slopes of the associated bacteria are
367 by far the steepest, corresponding to a predominant incorporation of ^{15}N, whereas non-
368 heterocystous cyanobacteria reveal flat slopes accompanying predominant incorporation of
369 ^{13}C (Table 2).

370

371 Table 2: Regression analyses of ^{13}C over ^{15}N uptake for the functional groups heterocystous
372 cyanobacteria (*Aphanizomenon* sp., *Dolichospermum* sp., *Nodularia* sp.), associated bacteria

373 (Alphaproteo and Cytophaga/Bacteroidetes bacteria), and non-heterocystous cyanobacteria
374 (*Pseudanabaena* sp.) for the different incubation times. Anova results display comparisons of
375 regression slopes of the different functional groups (ANCOVAs with and without interactions
376 between the factor (functional group) and the co-variable (^{15}N uptake) were calculated with
377 linear models, with ^{13}C uptake set as dependent variable. ANOVAs were then calculated
378 between both ANCOVAs to test for differences in the regression slopes).
379

Incubation time	*10 min*	*30 min*	*60 min*	*6 h*	*24 h*
Heterocystous cyanobacteria	Y=0.001+0.246x, R^2=0.88, p=0.000	Y=0.004-0.024x, R^2=0.00, p=0.308	Y=0.001+0.03x, R^2=0.16, p=0.000	Y=0.002+0.149x, R^2=0.82, p=0.000	Y=0.00+0.01x, R^2=0.56, p=0.000
Associated bacteria	Y=0.004+0.018x, R^2=0.02, p=0.471	Y=0.003+0.105x, R^2=0.45, p=0.06	Y=-0.02+1.94x, R^2=0.52, p=0.000	Y=0.004+0.329x, R^2=0.4, p=0.007	Y=0.015-0.022x, R^2=0.24, p=0.02
Non-heterocystous cyanobacteria	Y=0.004+0.028x, R^2=0.04, p=0.169	Y=0.003+0.105x, R^2=0.28, p=0.02	Y=0.004+0.05x, R^2=0.72, p=0.001	Y=0.003+0.117x, R^2=0.82, p=0.000	Y=0.009-0.002x, R^2=0.02, p=0.27
Anova	F=2.77, p=0.066	F=5.69, p=0.001	F=12.9, p=0.000	F=60.42, p=0.000	F=9.79, p=0.000

380

381 4. Discussion:

382 The present study determined the specific contribution of four different cyanobacterial species
383 and the two most abundant associated bacterial groups in carbon as well as nitrogen fixation
384 and cycling in late stage cyanobacterial bloom associations. Altogether, the cyanobacterium
385 *Pseudanabaena* spp. dominated the carbon assimilation as well as nitrogen fixation at the
386 early time-points, and the associated Alphaproteo- and Cytophaga/Bacteroidetes bacteria the
387 nitrogen cycling and possibly N_2 fixation at the later time-points. The filamentous,

388 heterocystous cyanobacteria *Nodularia* sp., *Dolichospermum* sp., and *Aphanizomenon* sp. on
389 the other hand, either showed no or erratic carbon and nitrogen uptake. Among the associated
390 heterotrophic bacteria Cytophaga/Bacteroidetes were more active in the carbon cycling,
391 whereas Alphaproteobacteria revealed higher activity in nitrogen cycling. However, high
392 intra-species variability was observed in all examined species, which partly impeded
393 significant differences in isotope uptake between species and time points.

394

395 4.1. Bi-carbonate uptake of cyanobacteria and associated heterotrophic bacteria

396 Surprisingly, *Pseudanabaena* sp. and not the heterocystous cyanobacteria was the most
397 prominent species in carbon assimilation (Fig. 3), with fixation rates up to 2.55 nmol C h^{-1} l^{-1}.
398 Indeed, carbon fixation rates of *Pseudanabaena* sp. were much higher than the rates for the
399 heterocystous species *Aphanizomenon* sp., *Dolichospermum* sp., and *Nodularia* sp. together
400 (Table 1, exception after 10 min of incubation due to 3 extraordinary high measurements in
401 *Nodularia* sp.). However, in combined measurements of June, July and August in the
402 preceding seasons 2012 and 2013, the three heterocystous species together accounted for ca.
403 5-250 nmol C h^{-1} l^{-1} (Klawonn et al., 2016). Thus, the heterocystous cyanobacteria still hold
404 key roles in carbon fixation in the Baltic Sea [14,37], with much higher fixation rates
405 compared to the estimated ones of *Pseudanabaena* sp. in the present study. In our case, the
406 appearance of the bloom and the curly phenotype of *Nodularia* sp. suggested a late stage of
407 the bloom (Fig. 4), and the low activity of *Aphanizomenon* sp., *Dolichospermum* sp., and
408 *Nodularia* sp. cells might be attributed to inactive cells at the late bloom stage.
409 *Pseudanabaena* sp. was still active and may be adapted to this situation where P-supply by
410 degrading blooms may be granted.

411 Measurements of heterotrophic bacteria at the later incubation times also revealed enhanced
412 $^{13}C/^{12}C$ ratios (Fig. 5), and heterotrophic bacteria may also incorporate bi-carbonate [38].

413 However, the ^{13}C signal in heterotrophic bacteria arises after 6 h incubation which may be
414 related to recycled organic carbon released by *Pseudanabaena* sp. and other cells. The higher
415 proportion of Cytophaga/Bacteroidetes bacteria in the incorporation of ^{13}C compared to
416 Alphaproteobacteria (Fig. 5) fits the current knowledge on their ecology: Marine
417 Cytophaga/Bacteroidetes are specialized in the degradation of high molecular weight
418 compounds (Fernández-Gómez et al., 2013; Kirchman, 2002; Alonso et al., 2012), which are
419 especially exuded in high quantities in late stage and senescent blooms (Mühlenbruch et al.
420 2018; Seymour et al., 2017; Pinhassi et al., 2004). Alphaproteobacteria on the other hand
421 preferentially use low molecular weight compounds such as amino acids [40] and may act
422 complementary to Bacteroidetes/Cytophaga in cyanobacterial bloom associations [39]. Thus,
423 the higher ^{13}C incorporation in Cytophaga/Bacteroidetes bacteria may display the recycling of
424 complex organic material whereas the lower signal in the Alphaproteobacteria account for the
425 incorporation of low molecular weight exudates.

426

427 4.2. $^{15}N_2$ uptake of cyanobacteria and associated heterotrophic bacteria

428 *Pseudanabaena* sp. showed $^{15}N_2$ incorporation after 30 min of incubation, and was the only
429 species with significantly increased $^{15}N/^{14}N$ ratios at this time. Further, it was the species with
430 the highest $^{15}N/^{14}N$ ratios after 60 min of incubation (Fig. 6). Until now, the non-
431 heterocystous *Pseudanabaena* sp. was not shown to be involved in fixation of atmospheric
432 nitrogen in the Baltic Sea [13,14], despite the presence of nitrogenase genes [15]. However,
433 picocyanobacteria and non-heterocystous filamentous species were suspected for nitrogen
434 fixation under specific conditions before [14]. Taking into account that *Pseudanabaena* sp.
435 was the only species with increased $^{15}N/^{14}N$ ratios at the early sampling points, our data
436 suggest an active N_2 fixation by *Pseudanabaena* sp., with fixation rates between 0.17 and 1.49
437 nmol N h^{-1} l^{-1} (Table 1). Thus, at this late stage of the bloom, *Pseudanabaena* sp. might have

been responsible for the input of reactive nitrogen in the multi-species associations and ultimately into the nitrogen cycle of the Baltic Sea. Indeed, if converted to per cell rates, nitrogen fixation of *Pseudanabaena* sp. appears low with up to 0.07 fmol N cell $^{-1}$ h^{-1} if compared to the heterocystous species *Nodularia spumigena* (11 fmol N cell^{-1} h^{-1}, Ploug et al., 2011) and *Aphanizomenon* sp. (1-11 fmol N cell^{-1} h^{-1}, Ploug et al., 2010). However, this difference might be attributed to the much smaller cell size of *Pseudanabaena* sp., and compensated by higher cell numbers. In a comparably study of a Baltic Sea cyanobacterial bloom, cumulative fixation rates for combined measurements of June, July and August of the heterocystous species *Dolichospermum* sp., *Nodularia* sp., and *Aphanizomenon* sp. were determined with ca. 0.5-80 nmol N l^{-1} h^{-1} [14], i.e. approximately one dimension above that of *Pseudanabaena* sp. alone in the present study. Likewise to the carbon fixation, the inexistent nitrogen fixation of the heterocystous species in our study may be attributed to different stages of the blooms, with most cells of heterocystous species being inactive at the late stage of the bloom (Figs. 5 and 6). Congenial to these results, early/mid-summer nitrogen fixation rates in the Baltic Sea were up to 30 times higher compared to late summer [8]. Thus, heterocystous cyanobacteria may still be the prime nitrogen fixers in the Baltic Sea [5,6], but the possible participation of *Pseudanabaena* spp. should not be neglected. If this temporal divided nitrogen fixation between different cyanobacterial species represents a general feature for the Baltic Sea needs to be investigated in consecutive studies.

The overall highest $^{15}N/^{14}N$ ratios by the associated bacteria after 6 and 24 h of exposure are surprising, taking the high abundance of diazotrophic cyanobacteria and the low ^{15}N incorporation of the hosts into account. Indeed, one would expect the converse role allocation, where associated heterotrophic bacteria reveal lower $^{15}N/^{14}N$ ratios than their diazotrophic hosts (Adam et al., 2016; Ploug et al., 2011). However, our high $^{15}N/^{14}N$ ratios were obtained after 6 and 24 h of incubation, and thus, similar to the ^{13}C incorporation, the associated

463 bacteria may have used recycled nitrogen that was originally fixed by cyanobacteria.
464 Supporting this assumption, heterotrophic microorganisms in cyanobacterial associations
465 dominated by *Aphanizomenon* sp. relied on recycled nitrogen [43], and *Aphanizomenon* sp.
466 was shown to release up to 35% of the fixed nitrogen as NH_4^+ [7]. However, direct cell to cell
467 transmission between hosts and associated bacteria was not indicated (see 3.2 and the linear
468 models), and release and transfer of newly fixed N_2 was not indicated at a similar experiment
469 during 12 h of incubation [14].

470 The role of heterotrophic bacteria in nitrogen fixation budgets for aquatic ecosystem were
471 recently brought into focus (Bentzon-Tilia et al., 2015; Farnelid et al., 2013), and might have
472 been underestimated in preceding studies [44–46]. As examples, heterotrophic organisms
473 dominated the nitrogen fixation in the South Pacific Gyre [45], and were also the principle
474 nitrogen fixing organisms in a Baltic Sea estuary [17]. Indeed, there are hints that the
475 associated bacteria in our study also performed nitrogen fixation themselves and not only used
476 nitrogen released from other cells: First, if the associated bacteria would only recycle nitrogen
477 that was fixed by other organisms, one would expect a dilution in the $^{15}N/^{14}N$ ratios from the
478 primary fixer to the secondary user [8,14,43], which is not the case (Figs. 6 and 7). Second,
479 already after 30 min heterotrophic bacterial cells possessed the overall highest $^{15}N/^{14}N$ ratios
480 (Fig. 7), and this fast incorporation indicates active nitrogen fixation. Third, many
481 Alphaproteobacteria (Delmont et al., 2018; Bentzon-Tilia et al., 2015; Farnelid et al., 2013)
482 and Cytophaga/Bacteroidetes bacteria [47] possess nitrogenase genes, and are capable of
483 nitrogen fixation. To validate heterotrophic nitrogen fixation we performed a gene functional
484 analysis with the 16S data of the associated bacteria using paprica - PAthway PRediction by
485 phylogenetIC plAcement [48]. In this analysis, however, only 1.2% of the associated bacteria
486 yielded the full pathway (via ferredoxin) for nitrogen fixation (Supplemental 3) which does
487 not support our assumption. Nevertheless, ecosystem key functions may be performed by low

488 abundant bacteria [49,50], and the per cell fixation rates of the associated bacteria were more
489 than one dimension higher compared to *Pseudanabaena* sp. (1.2 vs 0.07 fmol N h^{-1} $cell^{-1}$), and
490 in the same dimension as uptake rates for the much bigger heterocystous cyanobacteria (0.1 –
491 32.7 fmol N $cell^{-1}$ h^{-1}) in the Baltic Sea [14]. Thus, given the high abundances of associated
492 bacteria, heterotrophic nitrogen fixation might contribute significantly to bulk fixation at this
493 late stage bloom. At this stage of the bloom, senescent phytoplankton exhibit high exudation
494 and leaking rates (e.g. Mühlenbruch et al., 2018), and create an environment with high levels
495 of labile DOC that fuels heterotrophic nitrogen fixation [44,52,53]. This is corroborated with
496 the linear models, where bacteria associated to inactive, senescent hosts showed the highest
497 ^{15}N uptake (data not shown). However, until now prerequisites and regulation of heterotrophic
498 nitrogen fixation as well as principle contradictions as fixation in oxygenated waters and at
499 high nitrate and ammonium concentrations are poorly understood [44], and should move into
500 the focus of upcoming studies.

501

502 4.3. Relation of ^{13}C to ^{15}N uptake

503 Significant correlations between ^{13}C and ^{15}N uptake occurred in most species and at most time
504 points (Table 2), which is in accordance with similar studies from cyanobacterial blooms in
505 the Baltic Sea (e.g. Klawonn et al., 2016). Nevertheless, relations between carbon and
506 nitrogen uptake indicated specific tasks of functional groups (Fig 7, Table 2). *Pseudanabaena*
507 sp. (non-hetercystous cyanobacterium) clearly dominated the ^{13}C uptake (Fig. 5) throughout
508 the whole incubation period, but was also the first species with increased ^{15}N signals (Fig. 6).
509 For the $^{15}N/^{14}N$ ratios, however, *Pseudanabaena* sp. was outpaced by the associated bacteria
510 from 6 h incubation onwards (Fig. 6), and revealed much lower per cell fixation rates (see
511 above). Thus, the associated bacteria may have dominated the nitrogen cycling and possibly
512 fixation at the later sampling points. This specification of functional groups was corroborated

513 by significant different slopes in linear models calculated for correlations between ^{13}C and ^{15}N
514 uptake (Table 2). The formation of distinct functional groups by different species in late stage
515 bloom associations may ultimately result in the allocation of desired metabolic pathways to
516 every member in the association, including members unable to perform these tasks [54,55].
517 The concerted action of diverse ecological functions by different functional groups was also
518 proposed for a chlorophyte and its prokaryotic epiflora [56], and might be a general feature of
519 multi-species associations.

520

521 Acknowledgements: This work was supported by the Leibniz Association and a grant of the
522 Human Frontiers Science Program (RGP0020/2016). We thank Annett Grütmüller for
523 NanoSIMS measurements, the field station Askö laboratory for provision of lab space and
524 permission of experiments, Susanne Busch and Regina Hansen for phytoplankton counting,
525 and Joe Montoya for the provision of the Excel Sheet for calculations of uptake rates. The
526 SIMS instrument was funded by the German Federal Ministry of Education and Research
527 (BMBF), grant identifier 03F0626A.

528

529 References

530 1. Wasmund N. Occurrence of cyanobacterial blooms in the Baltic Sea in relation to
531 environmental conditions. Int Rev der gesamten Hydrobiol und Hydrogr. 1997;82:
532 169–184. doi:10.1002/iroh.19970820205

533 2. Wasmund N, Voss M, Lochte K. Evidence of nitrogen fixation by non-heterocystous
534 cyanobacteria in the Baltic Sea and re-calculation of a budget of nitrogen fixation. Mar
535 Ecol Prog Ser. 2001;214: 1–14. doi:10.3354/meps214001

536 3. Stal LJ, Staal M, Villbrandt M. Nutrient control of cyanobacterial blooms in the Baltic
537 Sea. Aquat Microb Ecol. 1999;18: 165–173.

538 4. Bianchi TS, Westman P, Rolff C. Cyanobacterial blooms in the Baltic Sea: Natural or
539 human induced? Limnol Oceanogr. 2000;43: 716–726.

540 5. Stolte W, Balode M, Carlsson P, Grzebyk D, Janson S, Lips I, et al. Stimulation of
541 nitrogen-fixing cyanobacteria in a Baltic Sea plankton community by land-derived
542 organic matter or iron addition. Mar Ecol Prog Ser. 2006;327: 71–82.

543 6. Wasmund N, Nausch G, Schneider B, Nagel K, Voss M. Comparison of nitrogen fixation
544 rates determined with different methods : a study in the Baltic Proper. Mar Ecol Prog
545 Ser. 2005;297: 23–31.

546 7. Ploug H, Musat N, Adam B, Moraru CL, Lavik G, Vagner T, et al. Carbon and nitrogen
547 fluxes associated with the cyanobacterium Aphanizomenon sp. in the Baltic Sea. ISME
548 J. Nature Publishing Group; 2010;4: 1215–23. doi:10.1038/ismej.2010.53

549 8. Ohlendieck U, Stuhr A, Siegmund H. Nitrogen fixation by diazotrophic cyanobacteria in
550 the Baltic Sea and transfer of the newly fixed nitrogen to picoplankton organisms. J
551 Mar Syst. 2000;25: 213–219. doi:10.1016/S0924-7963(00)00016-6

552 9. Cole JJ. Interactions between bacteria and algae in aquatic ecosystems. Annu Rev Ecol
553 Syst. 1982;13: 291–314.

554 10. Ramanan R, Kang Z, Kim B, Cho D, Jin L, Oh H, et al. Phycosphere bacterial diversity in
555 green algae reveals an apparent similarity across habitats. ALGAL. Elsevier B.V.;
556 2015;8: 140–144. doi:10.1016/j.algal.2015.02.003

557 11. Seymour JR, Amin SA, Raina J-B, Stocker R. Zooming in on the phycosphere: the

ecological interface for phytoplankton–bacteria relationships. Nat Microbiol. 2017;2: 17065. doi:10.1038/nmicrobiol.2017.65

12. Walsby AE, Hayes PK, Boje R, Walsby AE, Hayes PK, Boje R. The gas vesicles , buoyancy and vertical distribution of cyanobacteria in the Baltic Sea. Eur J Phycol. 1995;30: 87–94. doi:10.1080/09670269500650851

13. Bauersachs T, Schouten S, Compaore J, Wollenzien U, Stal LJ, Damste JSS. Nitrogen isotopic fractionation associated with growth on dinitrogen gas and nitrate by cyanobacteria. Limnol Oceanogr. 2009;54: 1403–1411.

14. Klawonn I, Nahar N, Walve J, Andersson B. Cell-specific nitrogen- and carbon-fixation of cyanobacteria in a temperate marine system (Baltic Sea). 2016;18: 4596–4609. doi:10.1111/1462-2920.13557

15. Acinas SG, Haverkamp THA, Huisman J, Stal LJ. Phenotypic and genetic diversification of Pseudanabaena spp. (cyanobacteria). ISME J. 2009;3: 31–46. doi:10.1038/ismej.2008.78

16. Farnelid H, Bentzon-Tilia M, Andersson AF, Bertilsson S, Jost G, Labrenz M, et al. Active nitrogen-fixing heterotrophic bacteria at and below the chemocline of the central Baltic Sea. ISME J. 2013;7: 1413–23. doi:10.1038/ismej.2013.26

17. Bentzon-Tilia M, Traving SJ, Mantikci M, Knudsen-Leerbeck H, Hansen JLS, Markager S, et al. Significant N 2 fixation by heterotrophs, photoheterotrophs and heterocystous cyanobacteria in two temperate estuaries. ISME J. 2015;9: 273–285. doi:10.1038/ismej.2014.119

18. Ploug H, Adam B, Musat N, Kalvelage T, Lavik G, Wolf-Gladrow D, et al. Carbon,

nitrogen and O(2) fluxes associated with the cyanobacterium Nodularia spumigena in the Baltic Sea. ISME J. Nature Publishing Group; 2011;5: 1549–58. doi:10.1038/ismej.2011.20

19. Willén T. Studies on the Phytoplankton of Some Lakes Connected with or Recently Isolated from the Baltic. Oikos. [Nordic Society Oikos, Wiley]; 1962;13: 169–199. doi:10.2307/3565084

20. Weinbauer MG, Fritz I, Wenderoth DF, Höfle MG. Simultaneous extraction from bacterioplankton of total RNA and DNA suitable for quantitative structure and function analyses. Appl Environ Microbiol. 2002;68: 1082–1087. doi:10.1128/AEM.68.3.1082

21. Herlemann DP, Labrenz M, Jürgens K, Bertilsson S, Waniek JJ, Andersson AF. Transitions in bacterial communities along the 2000 km salinity gradient of the Baltic Sea. ISME J. 2011;5: 1571–9. doi:10.1038/ismej.2011.41

22. Eigemann F, Schulz-Vogt HN. Stable and labile associations of microorganisms with the cyanobacterium Nodularia spumigena. Aquat Microb Ecol. 2019; 3354. doi:https://doi.org/10.3354/ame01918

23. Glöckner FO, Fuchs BM, Glo FO, Amann R. Bacterioplankton Compositions of Lakes and Oceans : a First Comparison Based on Fluorescence In Situ Hybridization Bacterioplankton Compositions of Lakes and Oceans : a First Comparison Based on Fluorescence In Situ Hybridization. 1999;

24. Acinas SG, Ferrera I, Sarmento H, Díez-Vives C, Forn I, Ruiz-Gonzàlez C, et al. Validation of a new catalysed reporter deposition-fluorescence in situ hybridization probe for the accurate quantification of marine Bacteroidetes populations. Environ

603 Microbiol. 2015;17: 3557–3569. doi:10.1111/1462-2920.12517

604 25. Pernthaler A, Pernthaler J, Amann R. Fluorescence In Situ Hybridization and Catalyzed
605 Reporter Deposition for the Identification of Marine Bacteria Fluorescence In Situ
606 Hybridization and Catalyzed Reporter Deposition for the Identification of Marine
607 Bacteria. 2002;68. doi:10.1128/AEM.68.6.3094

608 26. Musat N, Foster R, Vagner T, Adam B, Kuypers MMM. Detecting metabolic activities in
609 single cells, with emphasis on nanoSIMS. FEMS Microbiol Rev. 2012;36: 486–511.
610 doi:10.1111/j.1574-6976.2011.00303.x

611 27. Polerecky L, Adam B, Milucka J, Musat N, Vagner T, Kuypers MMM. Look@NanoSIMS -
612 a tool for the analysis of nanoSIMS data in environmental microbiology. Environ
613 Microbiol. 2012;14: 1009–1023. doi:10.1111/j.1462-2920.2011.02681.x

614 28. Montoya JP, Voss M, Kahler P, Capone DG. A Simple, High-Precision, High-Sensitivity
615 Tracer Assay for N(inf2) Fixation. Appl Environ Microbiol. 1996;62: 986–93. Available:
616 http://www.pubmedcentral.nih.gov/articlerender.fcgi?artid=1388808&tool=pmcentr
617 ez&rendertype=abstract

618 29. Carpenter J. New measurements of oxygen solubility in pure and natural water.
619 Limnol Oceanogr. 1966;11: 264–277.

620 30. Weiss R. The solubility of nitrogen, oxygen and argon in water and seawater. Deep
621 Res. 1970;17: 721–735.

622 31. Sveden JS, Adam B, Walve J, Nahar N, Sved JB, Musat N, et al. High cell-specific rates
623 of nitrogen and carbon fixation by the cyanobacterium Aphanizomenon sp. at low
624 temperatures in the Baltic Sea. FEMS Microbiol Ecol. 2015;91: 1–10.

doi:10.1093/femsec/fiv131

32. Heinänen AP. Bacterial numbers , biomass and productivity in the Baltic Sea: a cruise study. Mar Ecol Pro Ser. 1991;70: 283-290.

33. Kroer N, Jorgensen NOG, Coffin RB. Utilization of dissolved nitrogen by heterotrophic bacterioplankton: A comparison of three ecosystems. Appl Environ Microbiol. 1994;60: 4116–4123.

34. Mohr W, Grosskopf T, Wallace DWR, LaRoche J. Methodological underestimation of oceanic nitrogen fixation rates. PLoS One. 2010;5: e12583. doi:10.1371/journal.pone.0012583

35. Wannicke N, Benavides M, Dalsgaard T, Dippner JW, Montoya JP, Voss M. New Perspectives on Nitrogen Fixation Measurements Using 15N2 Gas. Front Mar Sci. 2018;5: 1–10. doi:10.3389/fmars.2018.00120

36. RStudio Team. RStudio: Integrated Development for R. Boston, MA URL http//www.rstudio.com/. 2015; 2015.

37. Stal LJ, Albertano P, Bergman B, Von Bröckel K, Gallon JR, Hayes PK, et al. BASIC: Baltic Sea cyanobacteria. An investigation of the structure and dynamics of water blooms of cyanobacteria in the Baltic Sea - Responses to a changing environment. Cont Shelf Res. 2003;23: 1695–1714. doi:10.1016/j.csr.2003.06.001

38. Hesselsoe M, Nielsen JL, Roslev P, Nielsen PH. Isotope Labeling and Microautoradiography of Active Heterotrophic Bacteria on the Basis of Assimilation of 14 CO 2 Isotope Labeling and Microautoradiography of Active Heterotrophic Bacteria on the Basis of Assimilation of 14 CO 2. 2005;71: 646–655. doi:10.1128/AEM.71.2.646

647 39. Fernández-Gómez B, Richter M, Schüler M, Pinhassi J, Acinas SG, González JM, et al.
648 Ecology of marine Bacteroidetes: a comparative genomics approach. ISME J. 2013;7:
649 1026–1037. doi:10.1038/ismej.2012.169

650 40. Kirchman DL. The ecology of Cytophagaâ€“Flavobacteria in aquatic
651 environments. FEMS Microbiol Ecol. 2002;39: 91–100. doi:10.1111/j.1574-
652 6941.2002.tb00910.x

653 41. Alonso C, Musat N, Adam B, Kuypers M, Amann R. HISH-SIMS analysis of bacterial
654 uptake of algal-derived carbon in the R??o de la Plata estuary. Syst Appl Microbiol.
655 Elsevier GmbH.; 2012;35: 541–548. doi:10.1016/j.syapm.2012.08.004

656 42. Ploug H, Adam B, Musat N, Kalvelage T, Lavik G, Wolf-gladrow D, et al. Carbon ,
657 nitrogen and O 2 fluxes associated with the cyanobacterium Nodularia spumigena in
658 the Baltic Sea. ISME J. Nature Publishing Group; 2011;5: 1549–1558.
659 doi:10.1038/ismej.2011.20

660 43. Adam B, Klawonn I, Svedén JB, Bergkvist J, Nahar N, Walve J, et al. N 2 -fixation,
661 ammonium release and N-transfer to the microbial and classical food web within a
662 plankton community. ISME J. 2016;10: 450–459. doi:10.1038/ismej.2015.126

663 44. Bombar D, Paerl RW, Riemann L. Marine Non-Cyanobacterial Diazotrophs: Moving
664 beyond Molecular Detection. Trends Microbiol. Elsevier Ltd; 2016;24: 916–927.
665 doi:10.1016/j.tim.2016.07.002

666 45. Halm H, Lam P, Ferdelman TG, Lavik G, Dittmar T, Laroche J, et al. Heterotrophic
667 organisms dominate nitrogen fixation in the South Pacific Gyre. 2012; 1238–1249.
668 doi:10.1038/ismej.2011.182

669 46. Delmont TO, Quince C, Shaiber A, Esen ÖC, Lee ST, Rappé MS, et al. Nitrogen-fixing
670 populations of Planctomycetes and Proteobacteria are abundant in surface ocean
671 metagenomes. Nat Microbiol. 2018;3: 804–813. doi:10.1038/s41564-018-0176-9

672 47. Inoue J, Oshima K, Suda W, Sakamoto M, Iino T, Noda S, et al. Distribution and
673 Evolution of Nitrogen Fixation Genes in the Phylum Bacteroidetes. Microbes Environ.
674 2015;30: 44–50. doi:10.1264/jsme2.ME14142

675 48. Bowman JS, Ducklow HW. Microbial Communities Can Be Described by Metabolic
676 Structure : A General Framework and Application to a Seasonally Variable , Depth-
677 Stratified Microbial Community from the Coastal West Antarctic Peninsula. 2015; 1–
678 18. doi:10.1371/journal.pone.0135868

679 49. Dawson W, Hör J, Egert M, Kleunen M Van, Pester M. A Small Number of Low-
680 abundance Bacteria Dominate Plant Species-specific Responses during Rhizosphere
681 Colonization. 2017;8: 1–13. doi:10.3389/fmicb.2017.00975

682 50. Benjamino J, Lincoln S, Srivastava R, Graf J. Low-abundant bacteria drive
683 compositional changes in the gut microbiota after dietary alteration. Microbiome;
684 2018; 1–13.

685 51. Mühlenbruch M, Grossart H-P, Eigemann F, Voss M. Phytoplankton-derived
686 polysaccharides in the marine environment and their interactions with heterotrophic
687 bacteria. Environ Microbiol. 2018;20: 2671–2685. doi:10.1111/1462-2920.14302

688 52. Bonnet S, Dekaezemacker J, Turk-kubo KA, Moutin T, Hamersley RM, Grosso O, et al.
689 Aphotic N 2 Fixation in the Eastern Tropical South Pacific Ocean. 2013;8: 1–14.
690 doi:10.1371/journal.pone.0081265

691 53. Moisander PH, Steppe TF, Hall NS, Kuparinen J, Paerl HW. Variability in nitrogen and
692 phosphorus limitation for Baltic Sea phytoplankton during nitrogen-fixing
693 cyanobacterial blooms. 2003;262: 81–95.

694 54. Graham LE, Knack JJ, Piotrowski MJ, Wilcox LW, Cook ME, Wellman CH, et al.
695 Lacustrine Nostoc (Nostocales) and associated microbiome generate a new type of
696 modern clotted microbialite. J Phycol. 2014;291: 280–291. doi:10.1111/jpy.12152

697 55. Frischkorn KR, Haley ST, Dyhrman ST. Coordinated gene expression between
698 Trichodesmium and its microbiome over day-night cycles in the North Pacific
699 Subtropical Gyre. ISME J. Springer US; 2018;12: 997–1007. doi:10.1038/s41396-017-
700 0041-5

701 56. Zulkifly S, Hanshew A, Young EB, Lee P, Graham ME, Graham ME, et al. The epiphytic
702 microbiota of the globally widespread macroalga Cladophora glomerata (Chlorophyta,
703 Cladophorales). Am J Bot. 2012;99: 1541–1552. doi:10.3732/ajb.1200161

704

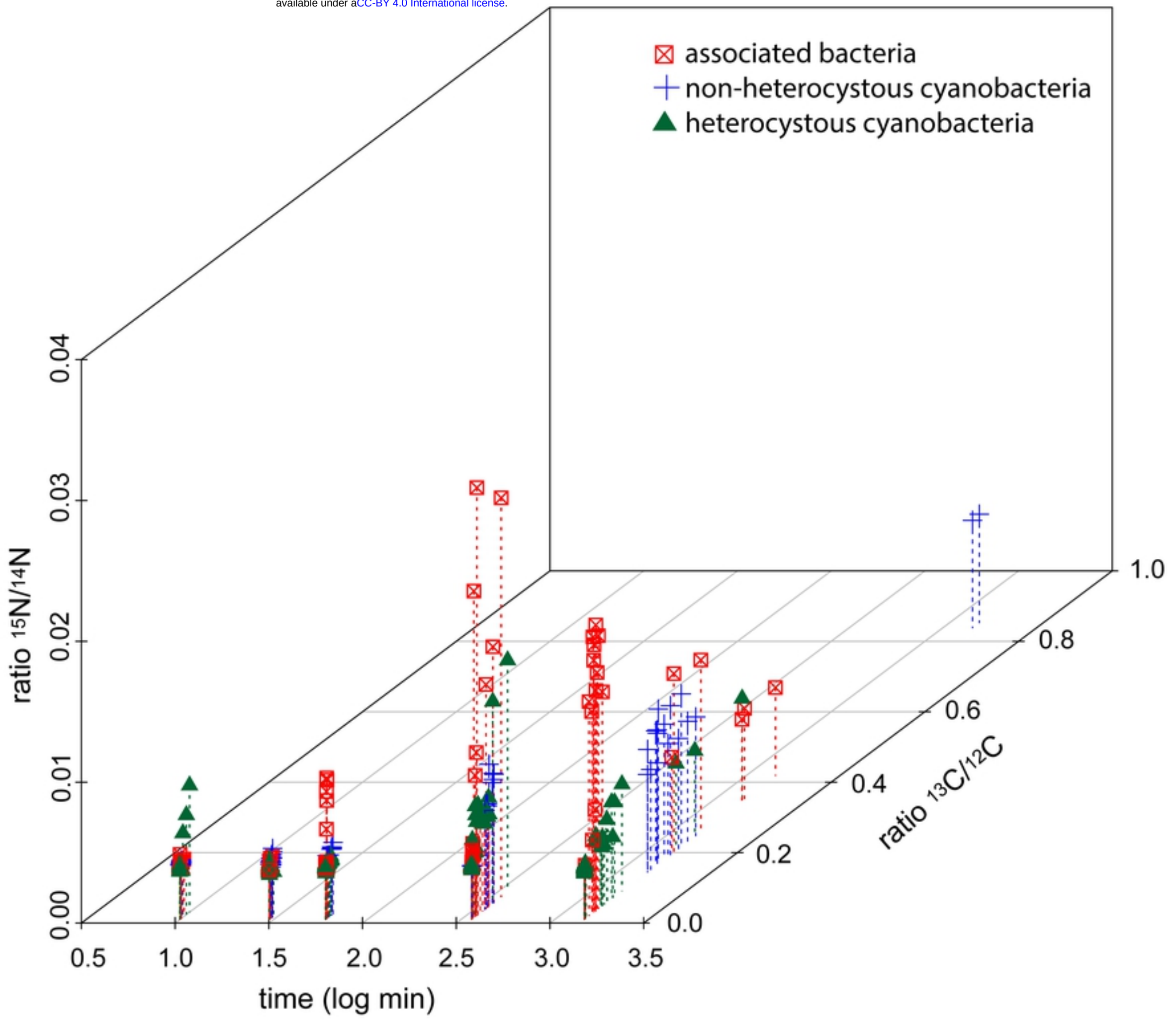

Fig. 7

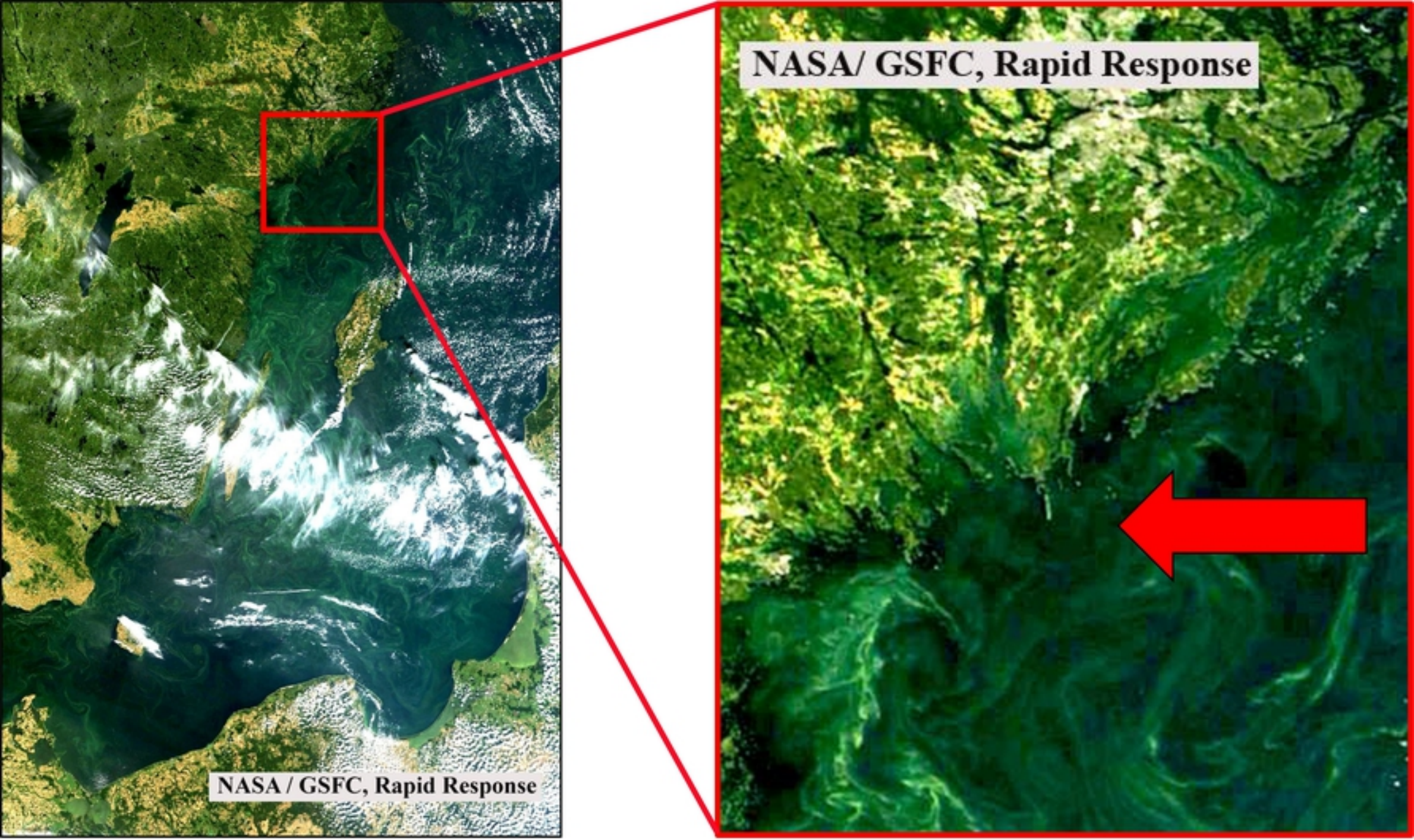

Fig. 1

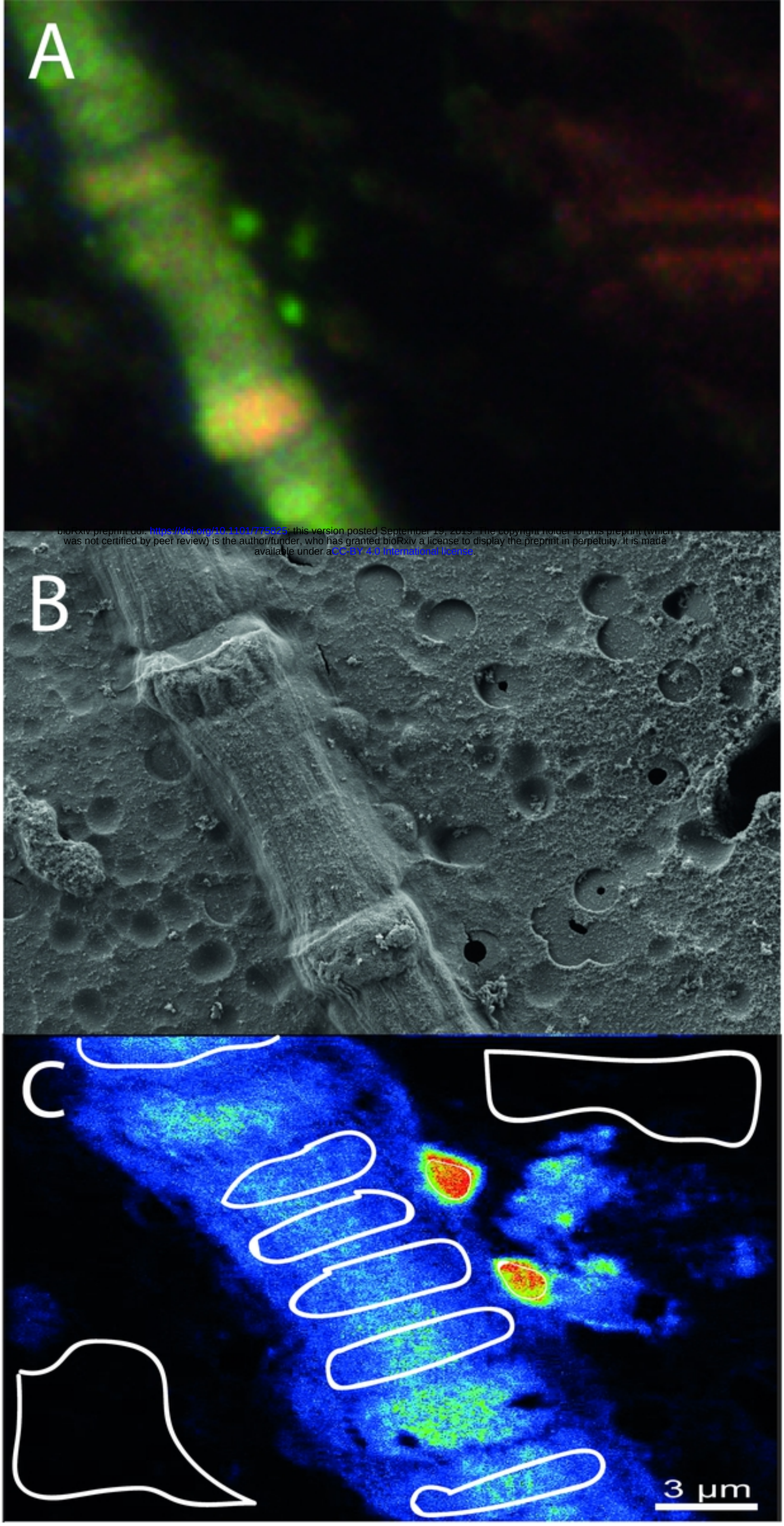

Fig. 2

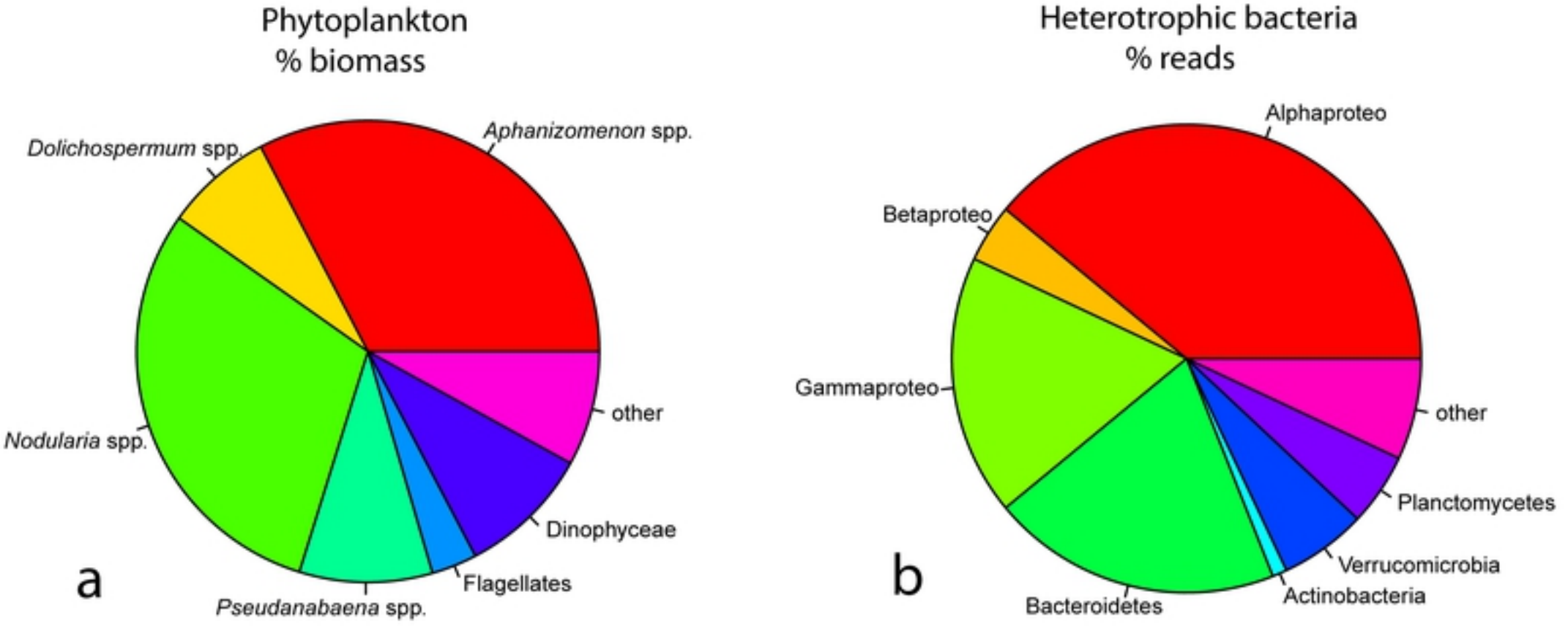
Phytoplankton
% biomass
Aphanizomenon spp.
Dolichospermum spp.
other
Nodularia spp.
Dinophyceae
Flagellates
Pseudanabaena spp.
a
Heterotrophic bacteria
% reads
Alphaproteo
Betaproteo
Gammaproteo
other
Planctomycetes
Verrucomicrobia
Actinobacteria
Bacteroidetes
b

Fig. 3

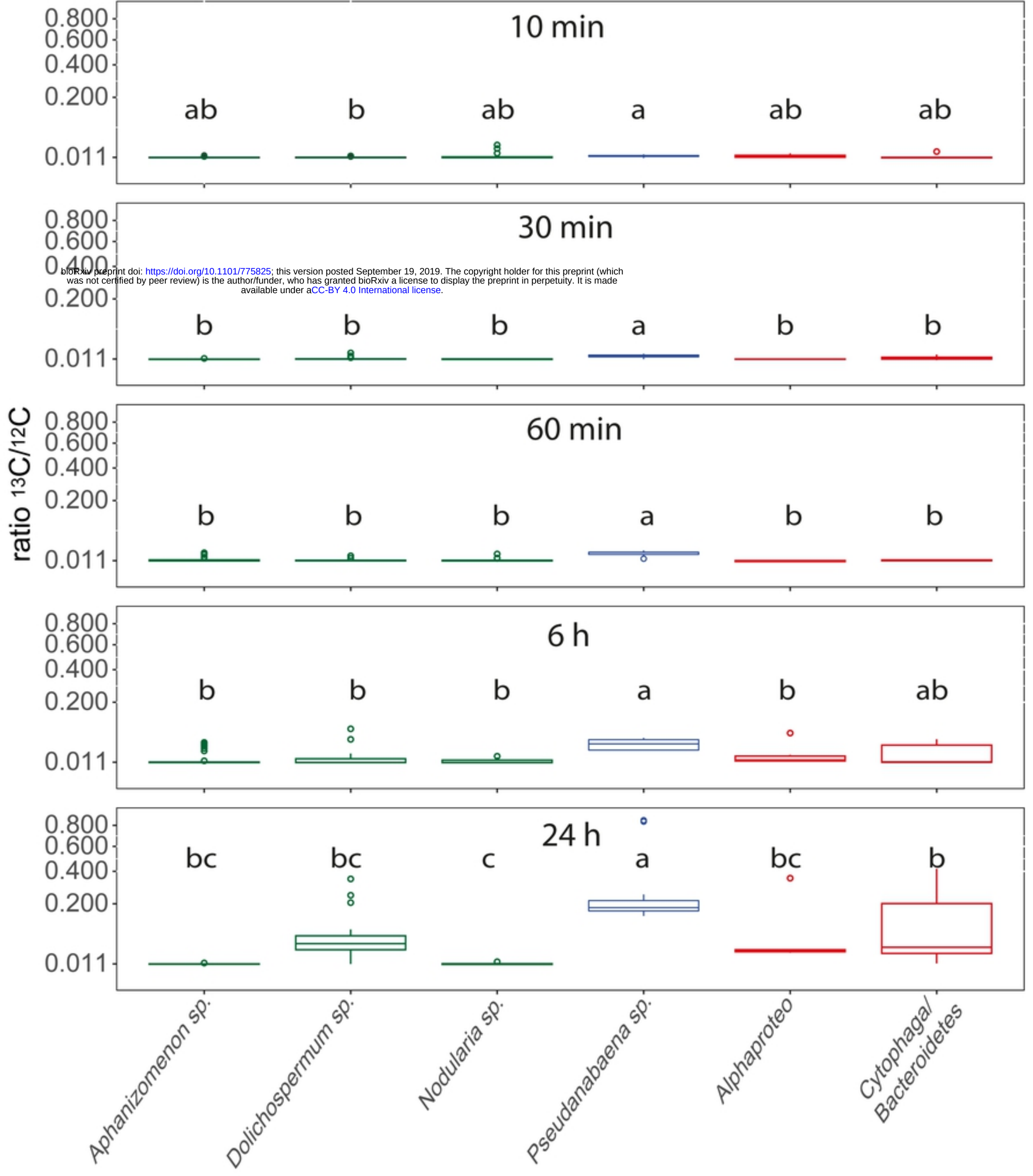

Fig. 5

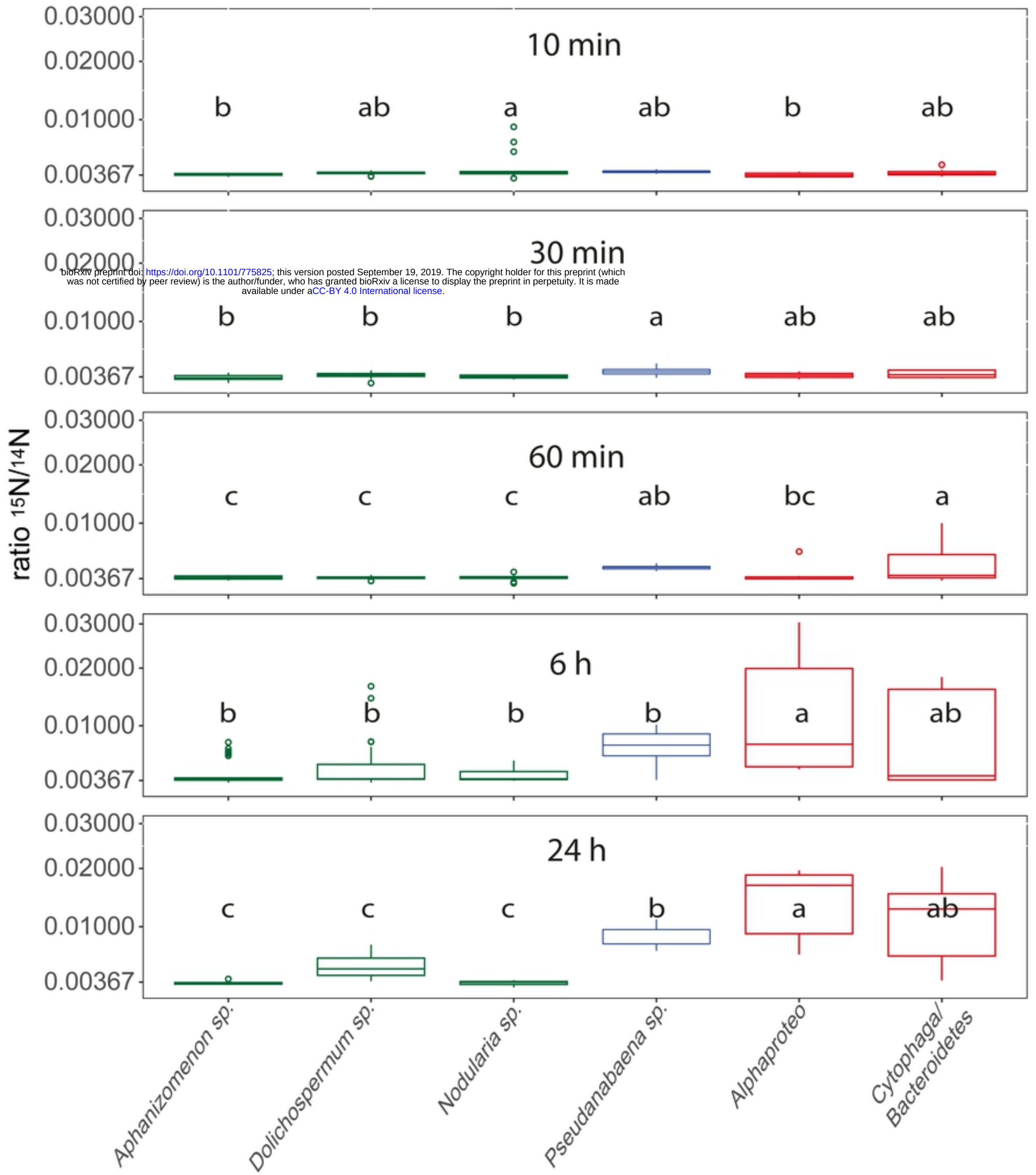

Fig. 6

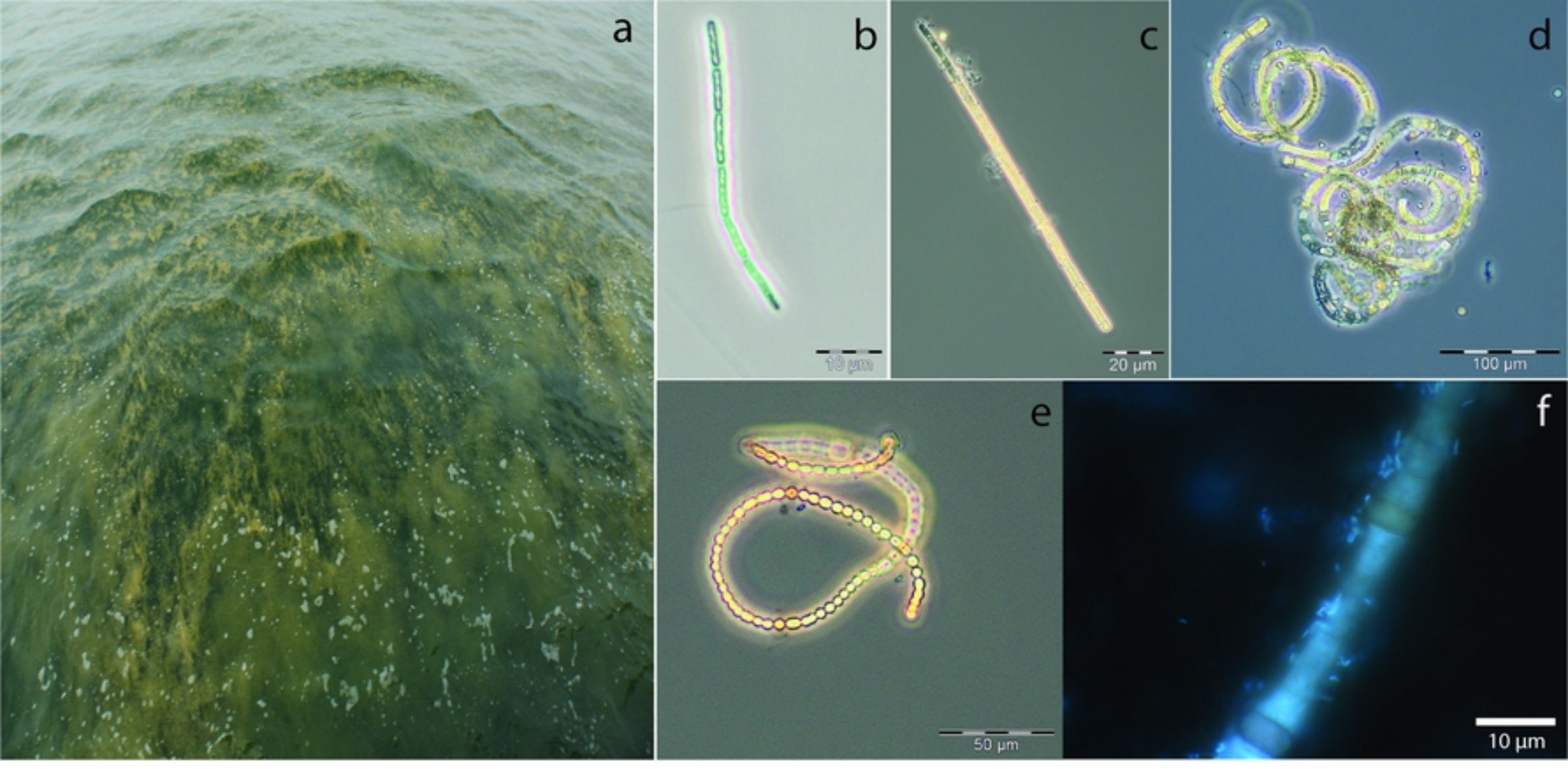

Fig. 4